北京应用物理与计算数学研究所
Institute of Applied Physics and Computational Mathematics

公开★

Smooth Particle Hydrodynamics Study on Ejecta Breakup and Size Distributions

Bao Wu

May 2024

Outline

- ✓ **Background**
- ✓ Numerical Methods
- ✓ Ejecta Breakup and Size distributions
- ✓ Conclusions

Shock-induced Micro-jet

- **Micro-jet phenomenon occurs on the metal surface under strong shock, forming high-speed and fine metal particles.**
- **Typical features: high-speed ~several km/s; small size ~ several μm**
- **Influencing factors: sensitive to shock strength, surface disturbances, material characteristics, micro-mesoscopic structural defects …, which are complex multi-mechanism dynamic behaviors.**

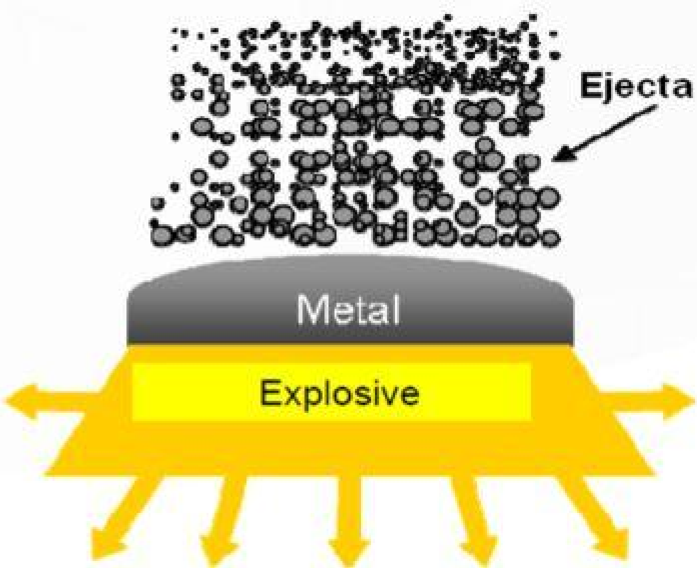

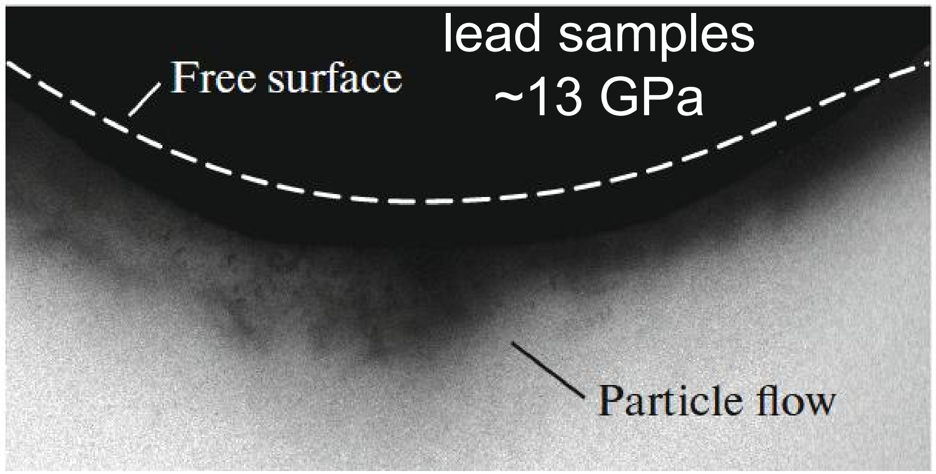

Ogorodnikov et al. Journal of Experimental and Theoretical Physics 2016

Formation mechanism

- Shock waves converge at the **surface disturbance interface**, resulting in the reverse of disturbance, resulting in the **formation of spike and bubble (RMI Mechanism)**;
- Micro-jet further broken up to form high-speed particles due to the velocity gradient along shock direction.

Metal surface machining defect

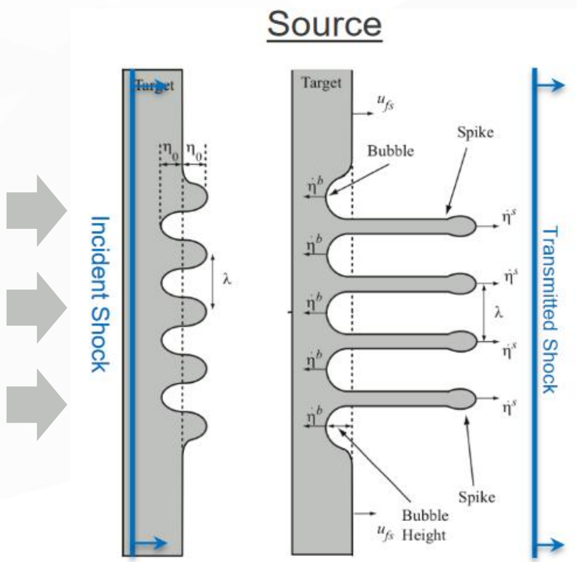

RMI Mechanism

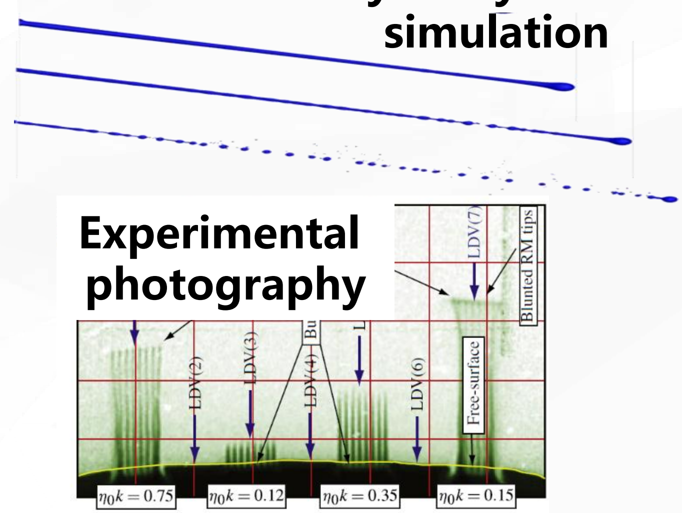

Formation and Breakup of Micro-jet

Buttler et al. Journal of Fluid Mechanics 2012

Research Backgroud

- The basic features of ejecta (high-speed ~several km/s; small size ~ several μm) bring great challenges to experimental diagnosis and theoretical research;
- Experiments (such as high-resolution holographic imaging technology) **cannot provide details on the dynamic process** of ejecta breakup;
- Molecular simulation **cannot give quantitative results comparable to the experimental scale**.

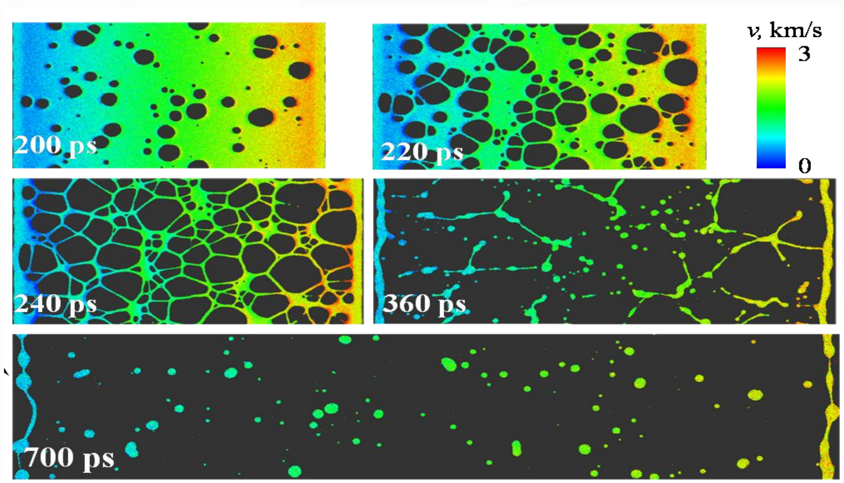

Molecular simulation

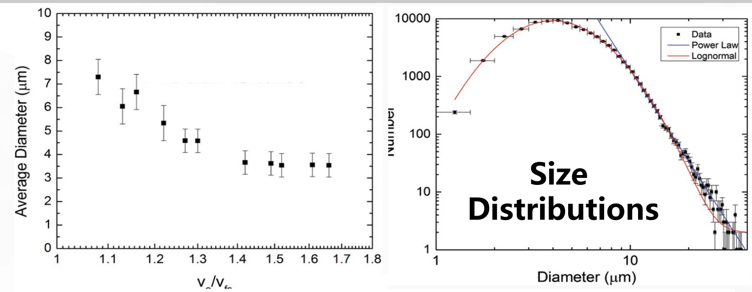

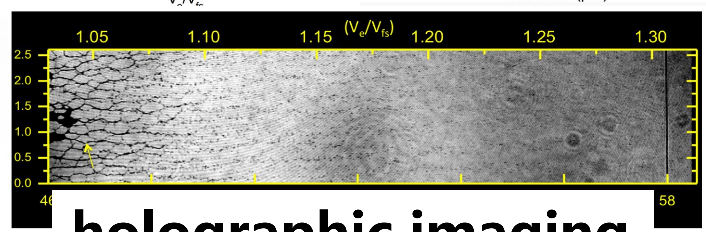

holographic imaging

Sorenson et al. Journal of Dynamic Behavior of Materials 2017

Outline

- ✓ Background
- ✓ **Numerical Methods**
- ✓ Ejecta Breakup and Size distributions
- ✓ Conclusions

Numerical Methods

- The scale of molecular simulation is several orders of magnitude different from that of the experiment;
- The mesh-based methods have difficulties in **describing large deformation and interfacial capture** (surface tension calculation);
- **The smooth particle hydrodynamics (SPH) are superior** in simulating large deformation and interfacial capture .

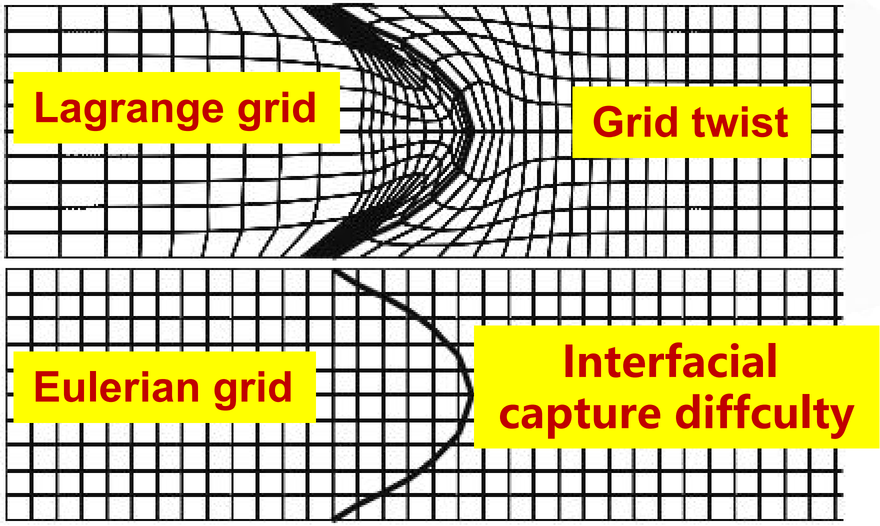

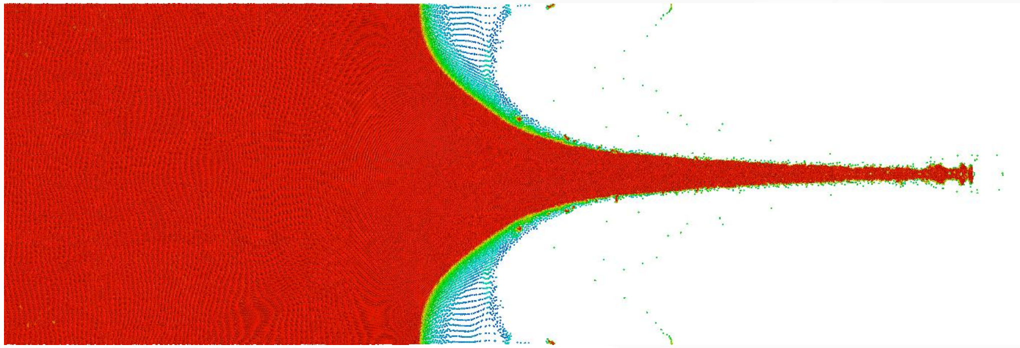

Ejection Simulated by SPH (2D)

Surface Tension

Continuous Surface Force (CSF) Model: $\boldsymbol{F}_i = -\sigma k_i \boldsymbol{n}_i \delta_{\Sigma,i}$

1) Surface normal: calculate according to the eigenvalue of the shape matrix;

$$\boldsymbol{n}_i = \begin{cases} -\dfrac{\nabla\lambda_i}{\|\nabla\lambda_i\|} & \text{if } \|\nabla\lambda_i\| > 0.1\dfrac{\lambda_i}{h_i}, \text{and } \lambda_i > 0.1 \\ \boldsymbol{0} & \text{otherwise,} \end{cases}$$

$$\nabla\lambda_i = \begin{cases} \sum_{j\in\Omega_i} (\lambda_j - \lambda_i)(\boldsymbol{L}_i \nabla W_{ij}) V_j & \text{if } \lambda_i \geq 0.7 \\ \sum_{j\in\Omega_i} \lambda_j (\boldsymbol{L}_i \nabla W_{ij}) V_j & \text{otherwise,} \end{cases}$$

2) Surface curvature: Local correction to avoid erroneous sharp areas;

$$\kappa_i = \sum_{j\in\Omega_i} s_{ij}(\boldsymbol{n}_j - \boldsymbol{n}_i)\cdot(\boldsymbol{L}_i \nabla W_{ij}) V_j,$$

$$s_{ij} = \begin{cases} 1 & \text{if } \boldsymbol{n}_i \cdot \boldsymbol{n}_j \geq -\dfrac{1}{3} \text{ and } \|\boldsymbol{n}_i\| > 0 \text{ and } \|\boldsymbol{n}_j\| > 0 \\ 0 & \text{otherwise,} \end{cases}$$

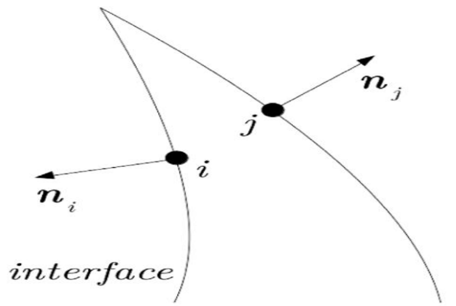

3) Interface function: Shepard correction is used to improve local accuracy.

$$\delta_{\Sigma,i} = 2\max\left(1, \frac{1}{2\sum_{j\in\Omega_i} W_{ij} V_j}\right) \left\| \sum_{j\in\Omega_i} \nabla W_{ij} V_j \right\|$$

Vergnaud et al. Computer Methods in Applied Mechanics and Engineering 2022

Numerical stability problem

- Non-uniform spatial distribution may lead to the **decline of calculation accuracy**, **cause stability problems in long-term calculation**;
- The particle shift technique (PST) and the diffusion term is to **keep uniform spatial distribution** and **suppress the non-physical oscillation** of the field variables.

PST method

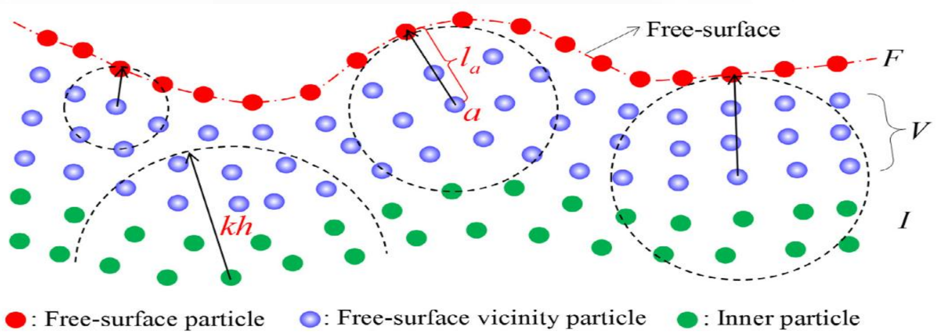

$$\delta \boldsymbol{x}_a = \begin{cases} 0 & \text{if } a \in F \\ -k_{\mathrm{CFL}} \cdot \mathrm{Ma} \cdot 2h^2 \cdot \sum_b \frac{m_b}{\rho_b} \chi_{ab} \nabla_a W_{ab}, \quad b \in [|\boldsymbol{x}_{ab}| < l_a] & \text{if } a \in V \\ -k_{\mathrm{CFL}} \cdot \mathrm{Ma} \cdot 2h^2 \cdot \sum_b \frac{m_b}{\rho_b} (1 + \chi_{ab}) \nabla_a W_{ab}, \quad b \in [|\boldsymbol{x}_{ab}| < kh] & \text{if } a \in I \end{cases}$$

Wang et al. Computer Methods in Applied Mechanics and Engineering 2019

Antuono et al. Computer Physics Communications 2010

Diffusion term

Mass conservation

$$\boldsymbol{\psi}_{ij} = 2(\rho_j - \rho_i) \frac{\boldsymbol{r}_{ji}}{|\boldsymbol{r}_{ij}|^2}$$

momentum conservation

$$\pi_{ij} = \frac{(\boldsymbol{u}_j - \boldsymbol{u}_i) \cdot \boldsymbol{r}_{ji}}{|\boldsymbol{r}_{ij}|^2}$$

Energy conservation

$$\boldsymbol{\phi}_{ij} = 2(e_j - e_i) \frac{\boldsymbol{r}_{ji}}{|\boldsymbol{r}_{ij}|^2}$$

Surface Detection (for PST)

PST needs to zero the normal shift at surface to ensure strict boundary conditions

Three-step Calculation of Interface Detection:

1) **Preliminary identification: obtain surface normal;**
2) **Geometric detection: scan the sector area to identify surface and internal particles;**
3) **Partition: Particles are divided into disperse particles, surface particles, near-surface particles, and internal particles.**

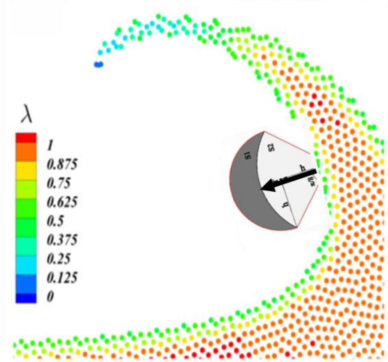

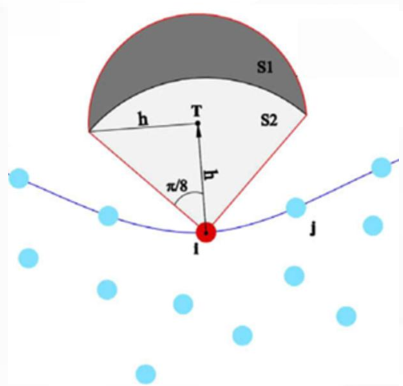

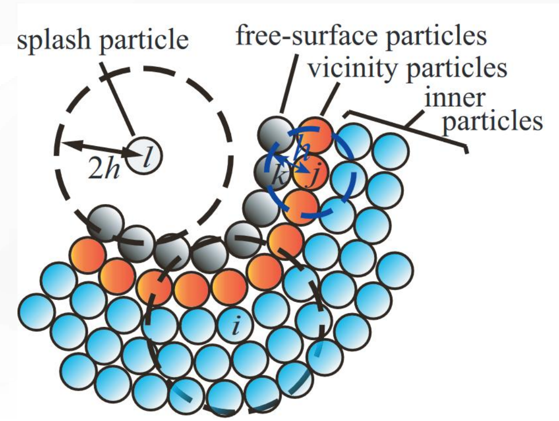

$$
\boldsymbol{n}_i = \begin{cases} -\dfrac{\nabla\lambda_i}{\parallel \nabla\lambda_i \parallel} & \text{if } \parallel \nabla\lambda_i \parallel > 0.1\dfrac{\lambda_i}{h_i}, \text{ and } \lambda_i > 0.1 \\ \mathbf{0} & \text{otherwise,} \end{cases}
$$

$$
\begin{cases} \forall j \in \mathbb{N}\left[\left|\boldsymbol{x}_{ji}\right| \geqslant \sqrt{2}\boldsymbol{h}, \left|\boldsymbol{x}_{jT}\right| < \boldsymbol{h}\right] & \boldsymbol{i} \notin \mathbb{F} \\ \forall j \in \mathbb{N}\left[\left|\boldsymbol{x}_{ji}\right| < \sqrt{2}\boldsymbol{h}, \left|\boldsymbol{n}\cdot\boldsymbol{x}_{jT}\right| + \left|\boldsymbol{\tau}\cdot\boldsymbol{x}_{jT}\right| < \boldsymbol{h}\right] & \boldsymbol{i} \notin \mathbb{F} \\ \text{otherwise} & \boldsymbol{i} \in \mathbb{F} \end{cases}
$$

Marrone et al. Journal of Computational Physics 2010
Khayyer et al. Journal of Computational Physics 2017

Numerical stability problem

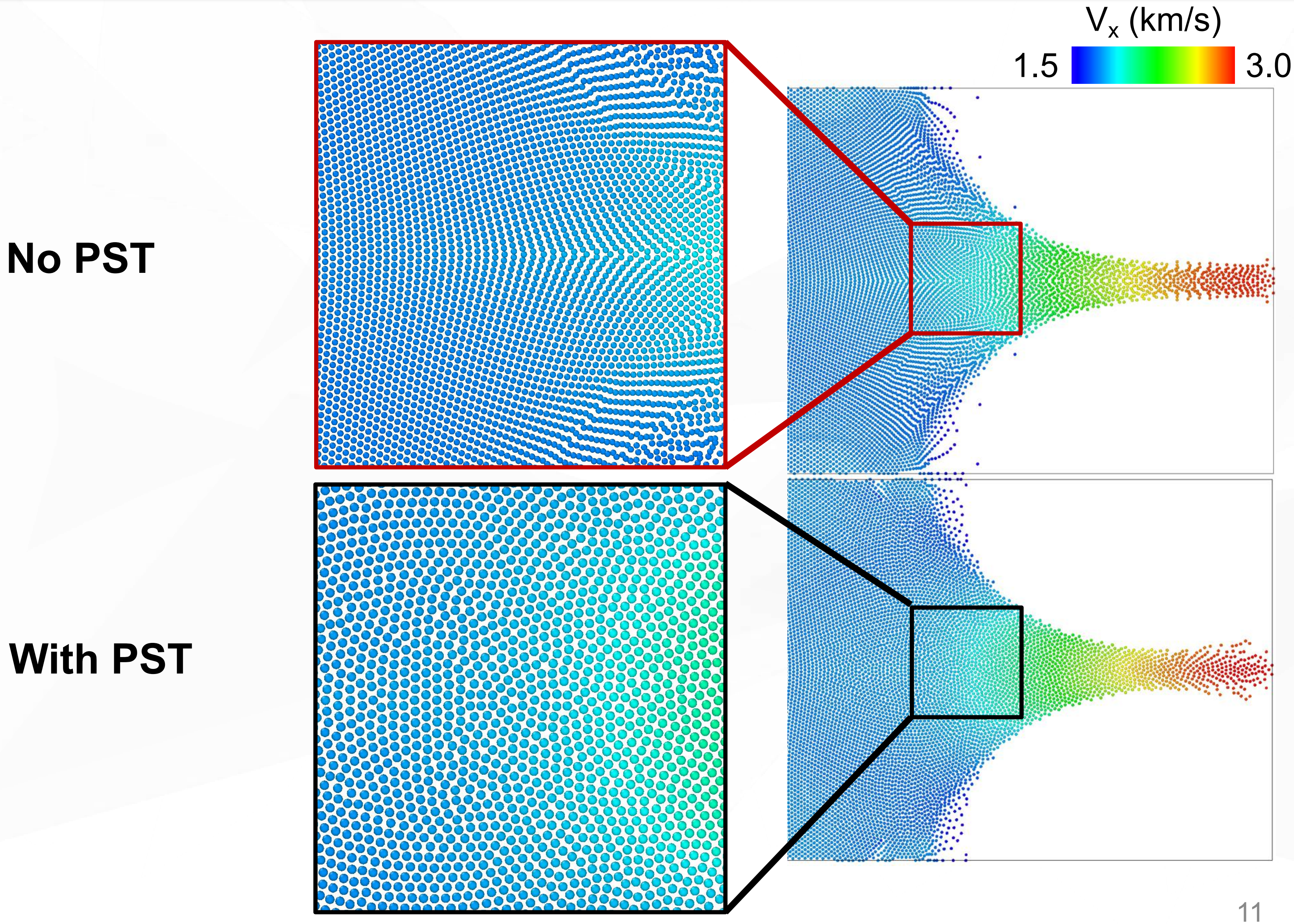

Verification-Metal Strength Effect

- **Problem Statement**: How does metal strength affect jet velocity?
- **Simulation settings**: copper surface trench wavelength 550 μ m, perturbation kh = {0.12, 0.35, 0.75, 1.5}, impact strength ~ 36GPa;
- **Verification**: SPH simulation can effectively evaluate the spike growth with strength effect.

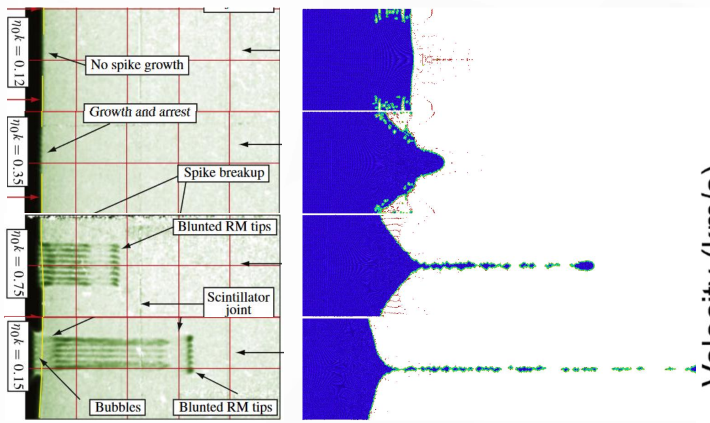

Jet Evolution
Left: Experiments
Right: SPH simulations

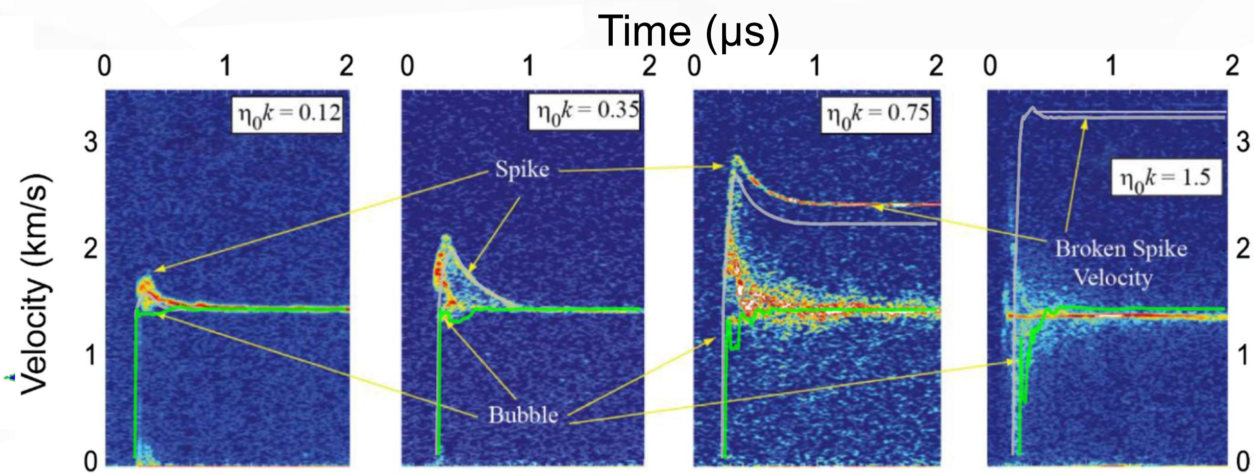

Comparison of Experimental and SPH Simulated Results of Jet Velocity

Buttler et al. Journal of Fluid Mechanics 2012

Verification-Droplet Oscillation

- **Problem Statement:** oscillation of spherical droplet in the initial velocity field;
- **Simulation settings:** radius of 0.005 m, density of 1000 kg/m³, surface tension coefficient of 0.2 ,initial velocity field (− Ax, − Ay, 2Az) with A = 5;
- **Verification:** The oscillation period is in good agreement with the theoretical solution.

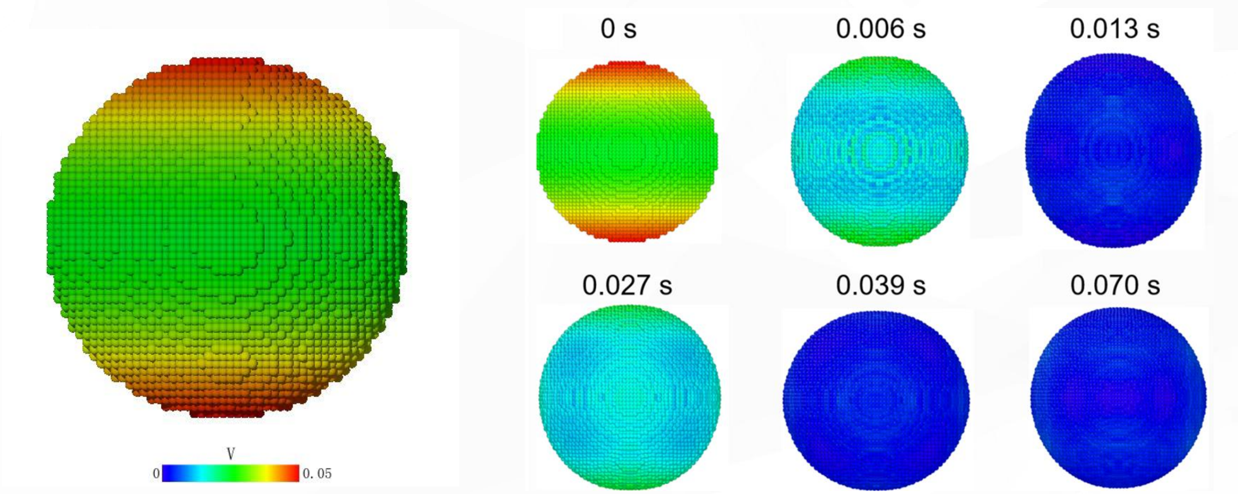

velocity field

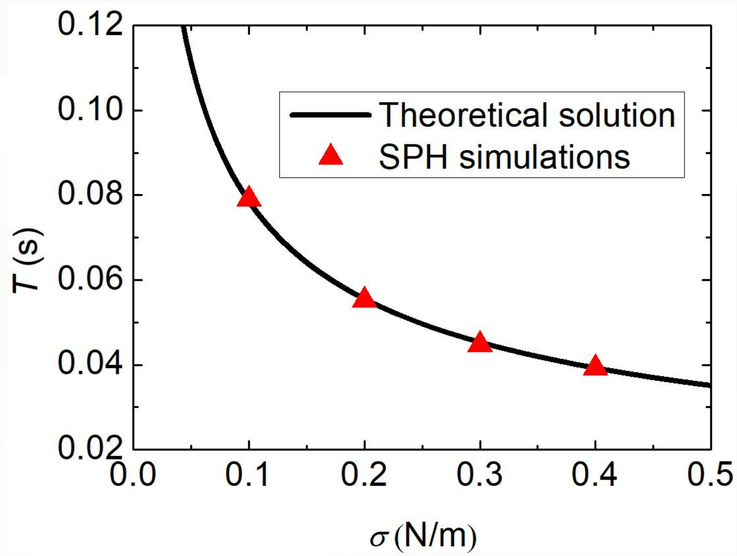

oscillation period vs surface tension coefficient

Verification--Rayleigh Instability of Cylindrical Rod

- **Problem Statement:** Rayleigh instability occurs in a stationary slender cylindrical rod;
- **Simulated settings:** Radius of 0.005 m and length of 2 m, density 1000 kg/m3, and the surface tension coefficient is 0.0728 N/m;
- **Verification:** the principal instability mode obtained is kR_0 = 0.694, close to theoretical solution of 0.697.

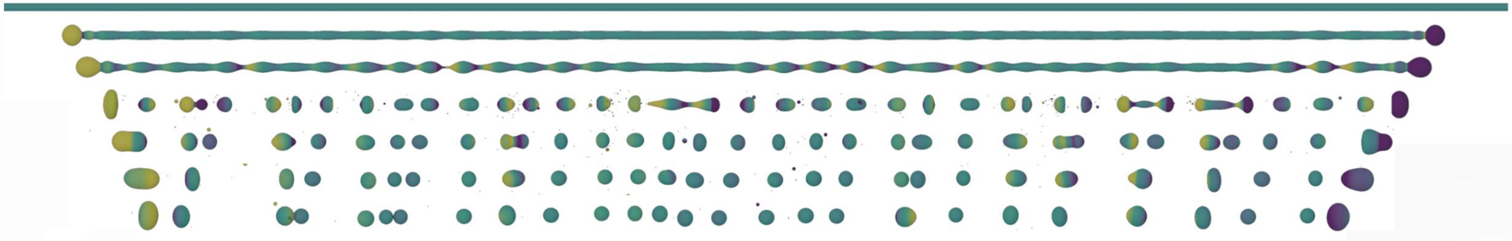

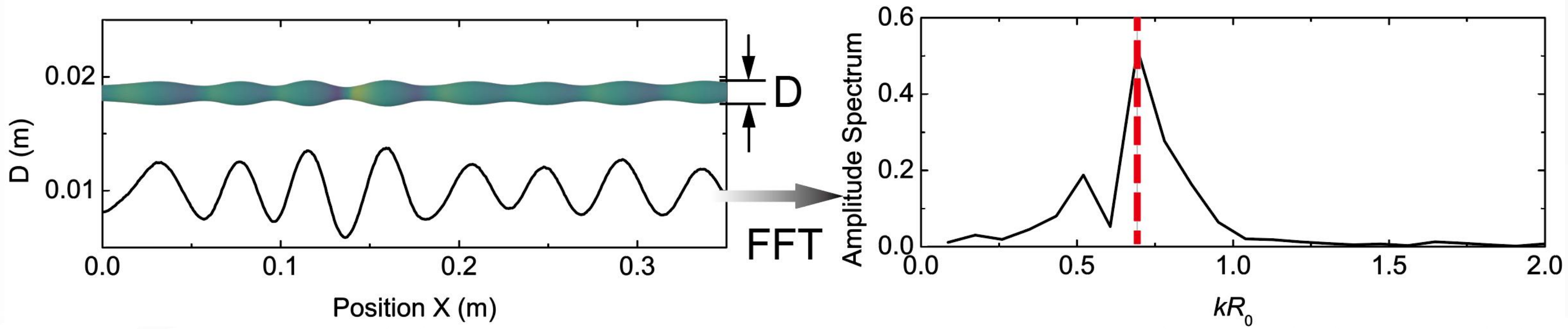

Outline

- ✓ Background
- ✓ Numerical Methods
- ✓ **Ejecta Breakup and Size distributions**
- ✓ Conclusions

Numerical Simulation of Jet Breakup

- **Simulation strategy:** a compressible form of conservation equation is required for shock induced ejection formation in early time, while the breakup stage adopt the weak compressibility assumption to speedup simulation;
- **Setting:** triangular groove (120 degree), impact pressure of ~ 20 GPa (total ~ 130 million particles).

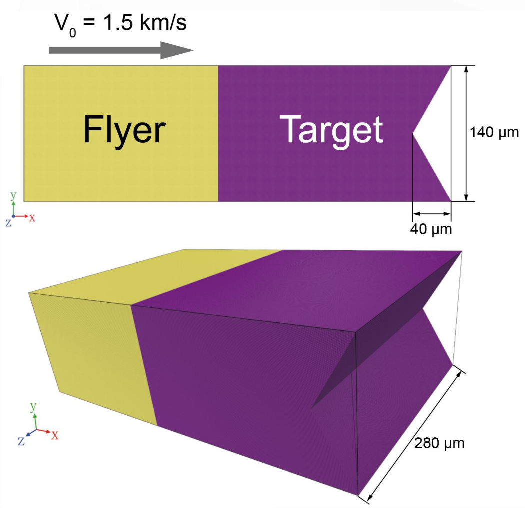

初始模型

射流形成与破碎过程

Breakup initiation-hole nucleation

- When the local thickness of the jet is close to the particle resolution, local penetration will occur randomly to form initial holes;

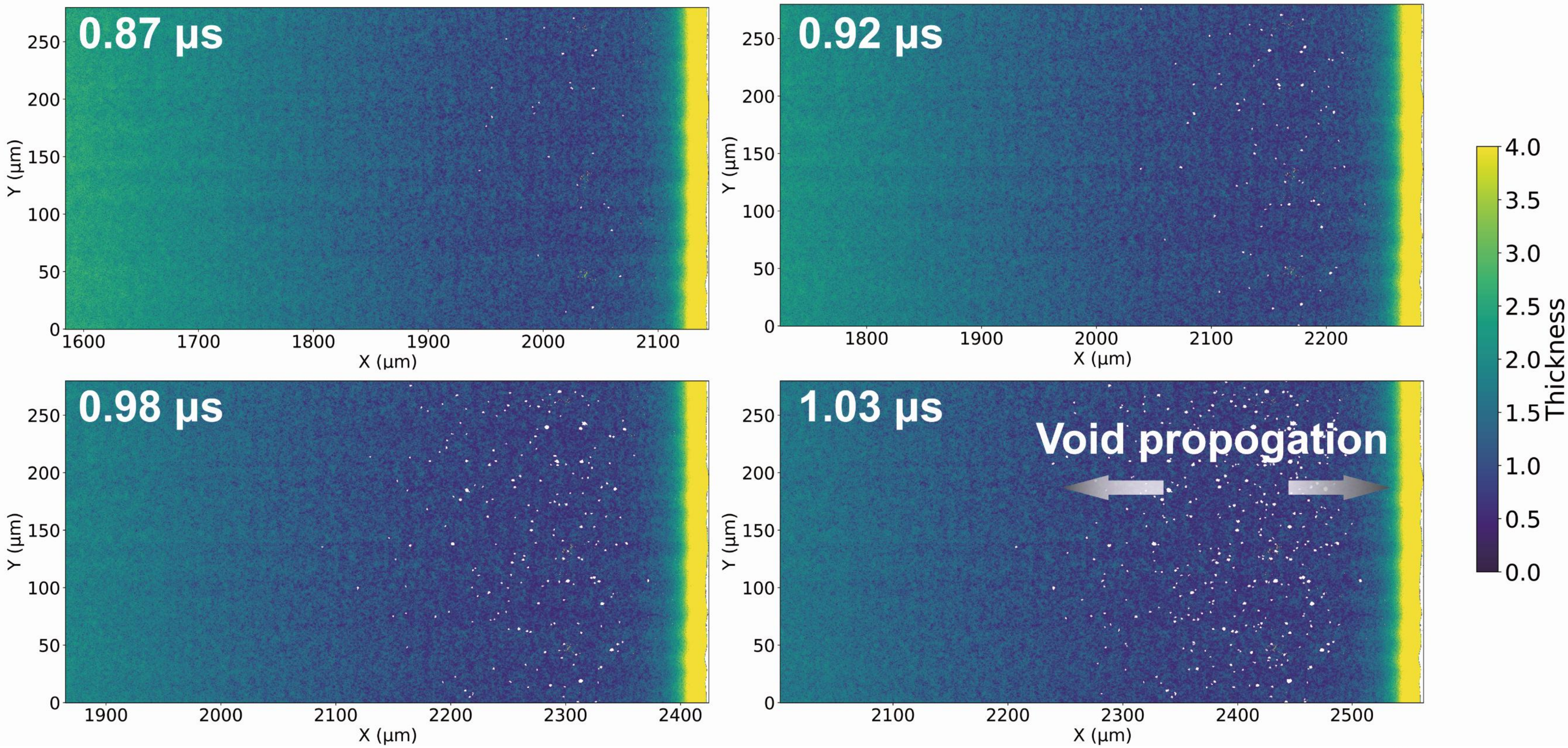

Broken zone propagation

- The perturbation generated by the holes then propagates inward

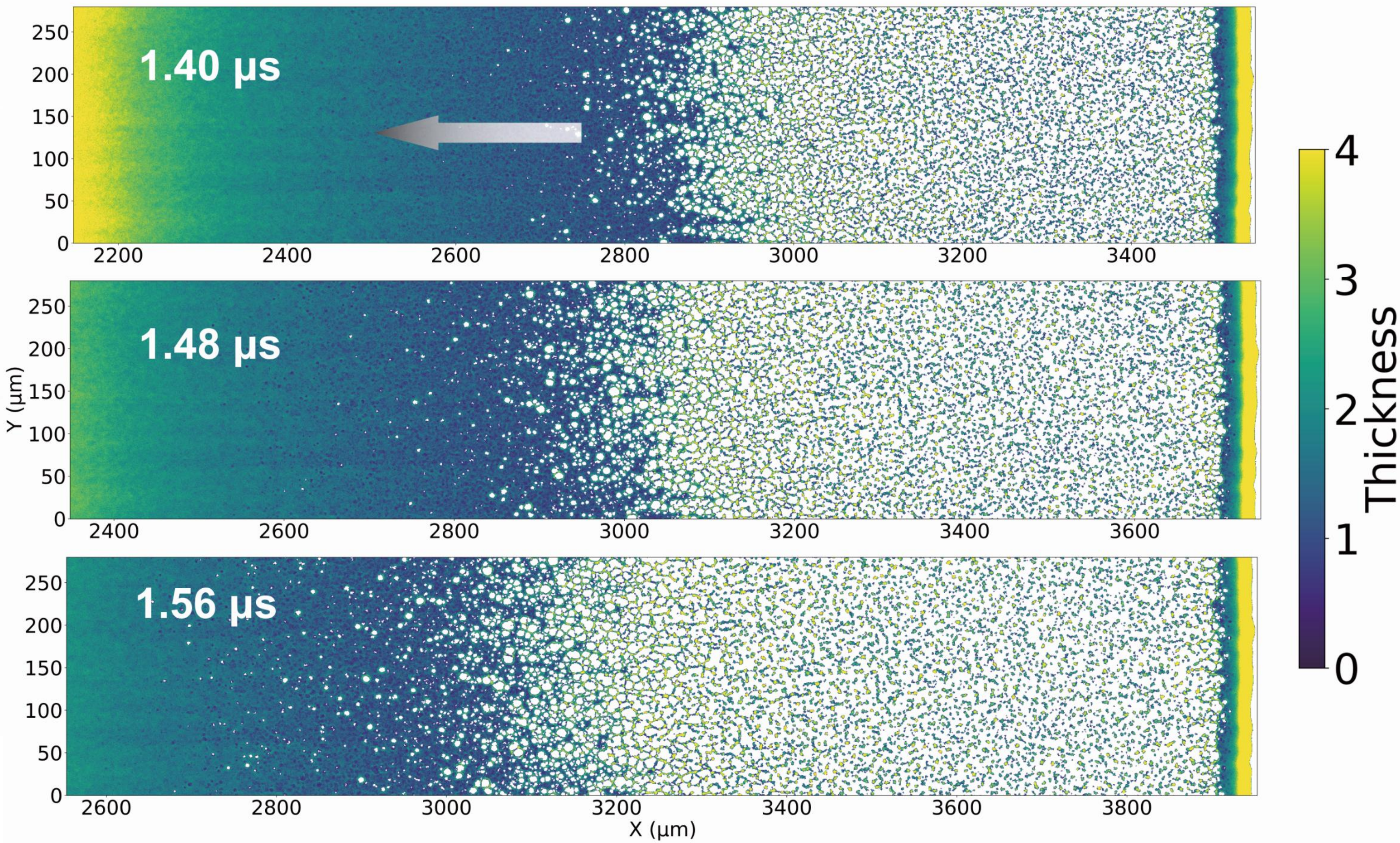

hole expansion

- The expansion of holes leads to the concentration of matter in the circular region, forming Rim structures.
- Hole growth can be simplified as the expansion of circular pores in stationary liquid films, and the expansion rate is given by :

$$v = \sqrt{\frac{2\sigma}{\rho h}},$$

Theoretical： 8.4 m/s

Simulated： 9.1 m/s ， 10.2 m/s

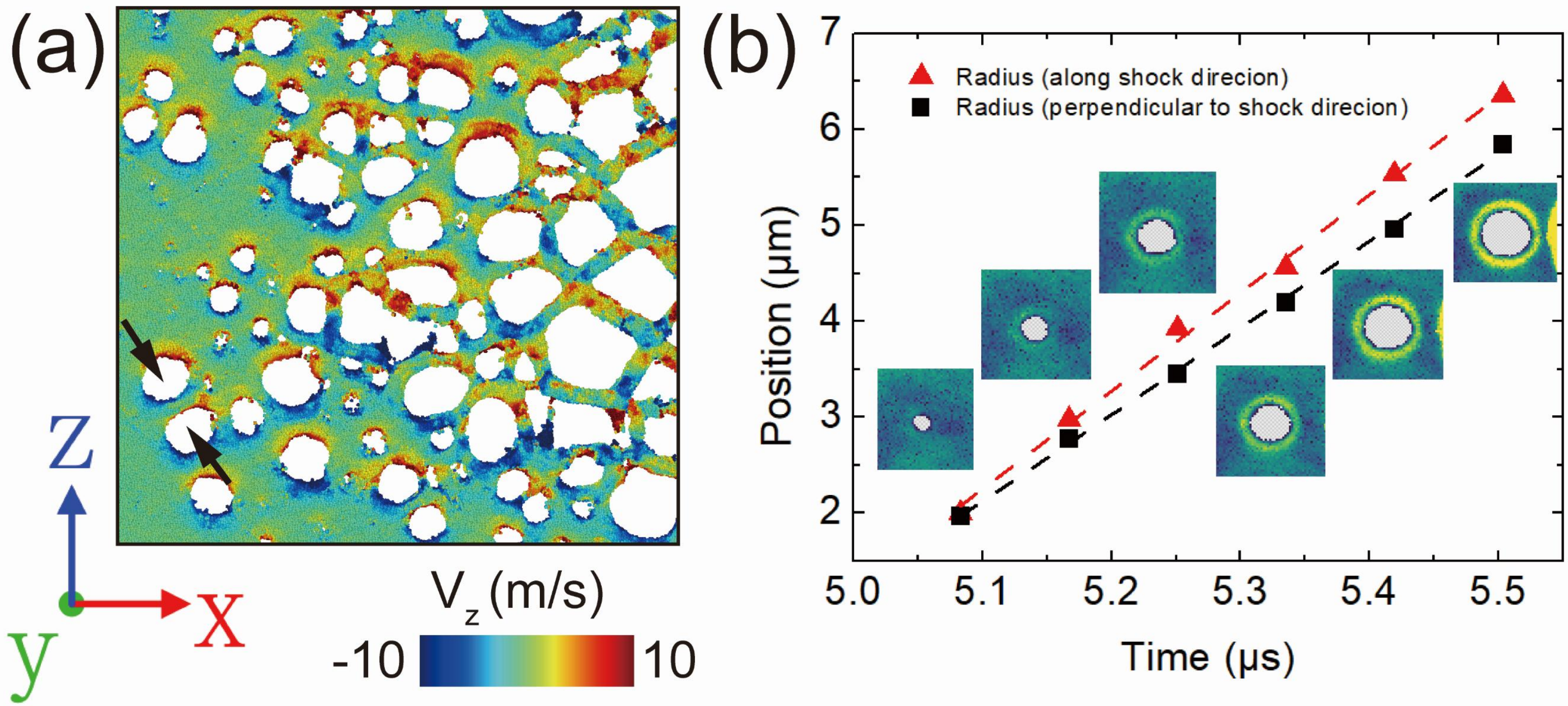

Dynamic process of breakup

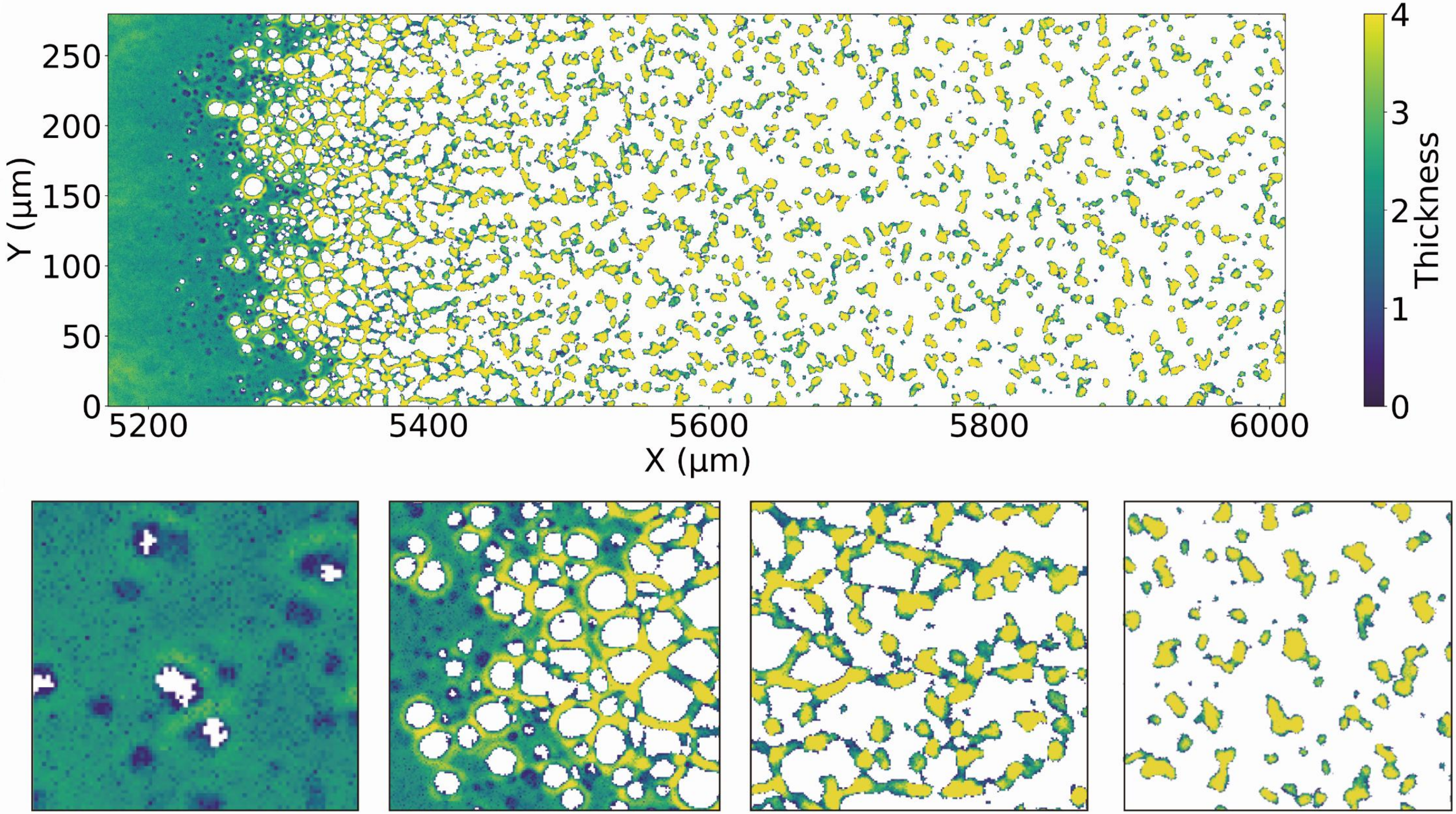

Hole nucleation

Hole growth
and network formation

network breakup
into filaments

filaments breakup
into particles

Second breakup

After the droplets are seprated from the strip structure, second breakup will occur:

- the oscillating fragmentation caused by the uneven internal velocity distribution of the droplets;
- the mutual collision between the droplets and triggers breakup.

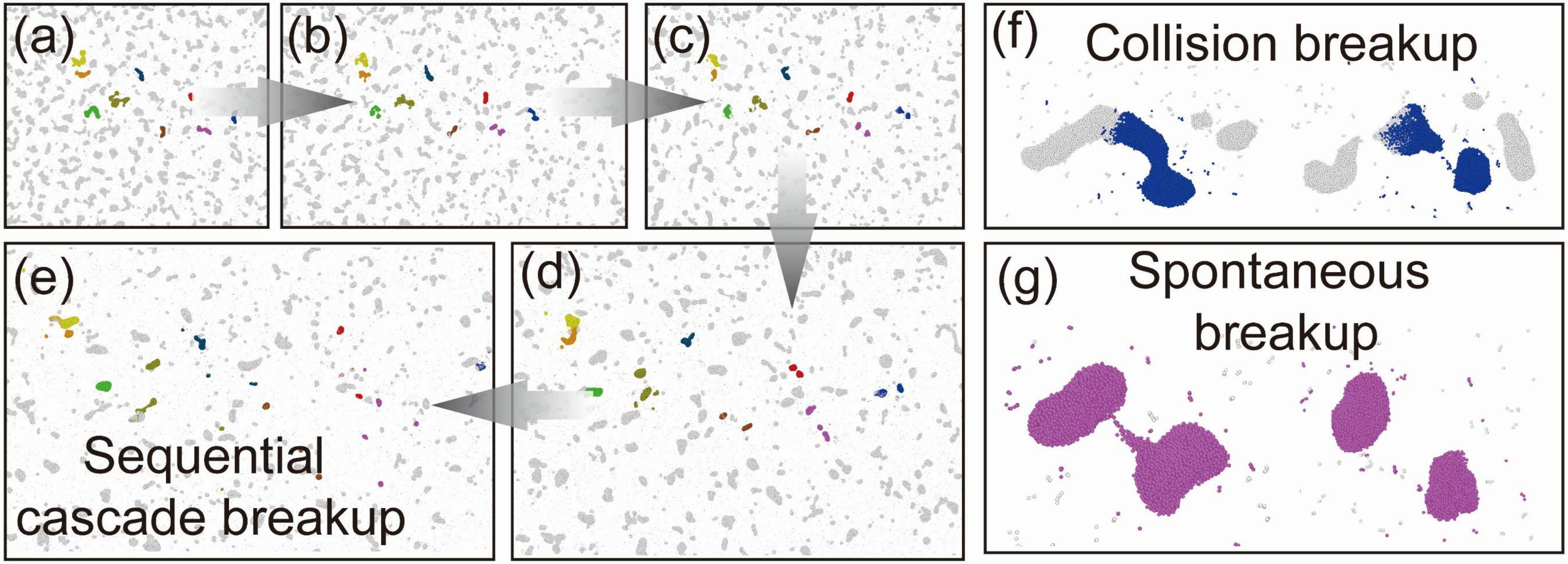

Statistics on particle breakup

- The Second breakup leads to the reduction of large-scale particles and the increase of small-scale particles;
- The distribution szie of particles is narrowed.

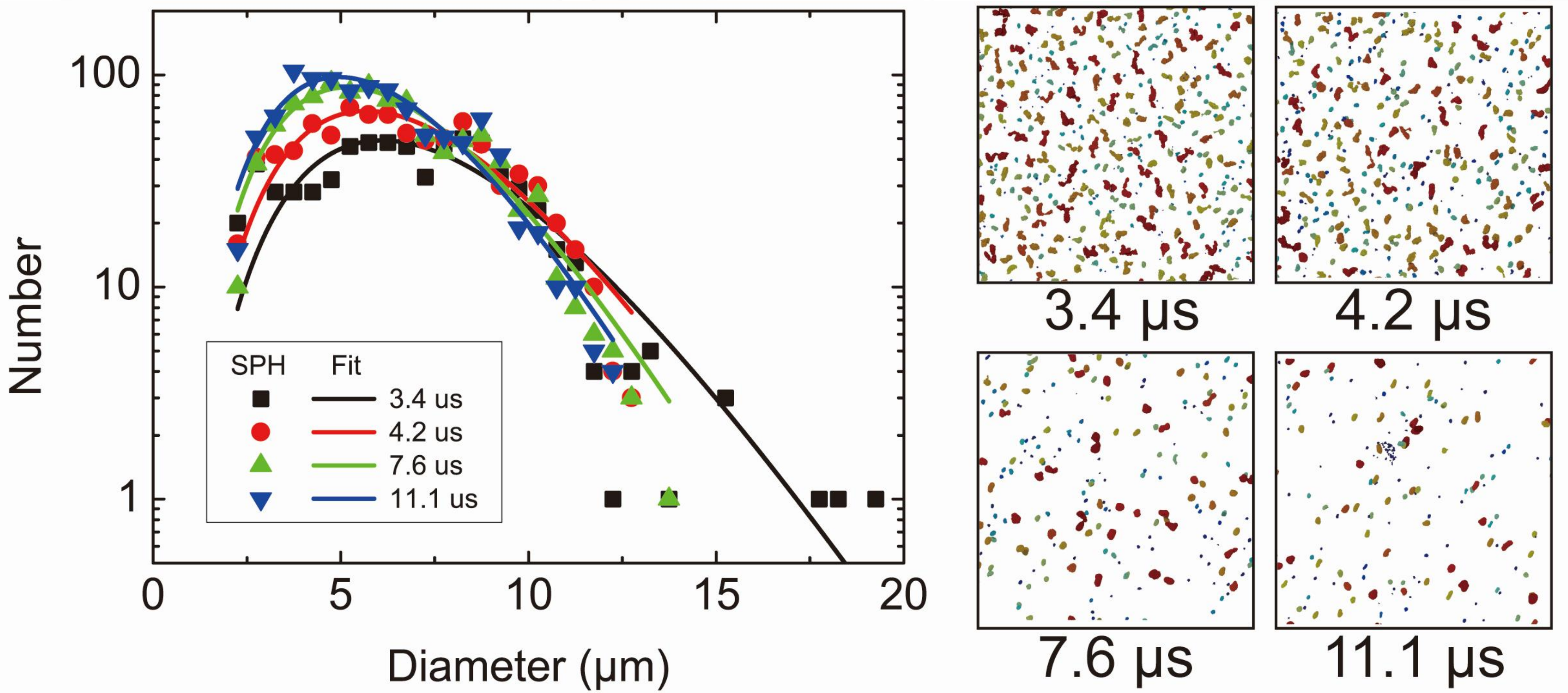

Size Distributions in Different Spatial Regions

- the distribution range of particles narrows with the increase of spatial distance (or ejecta velocity)

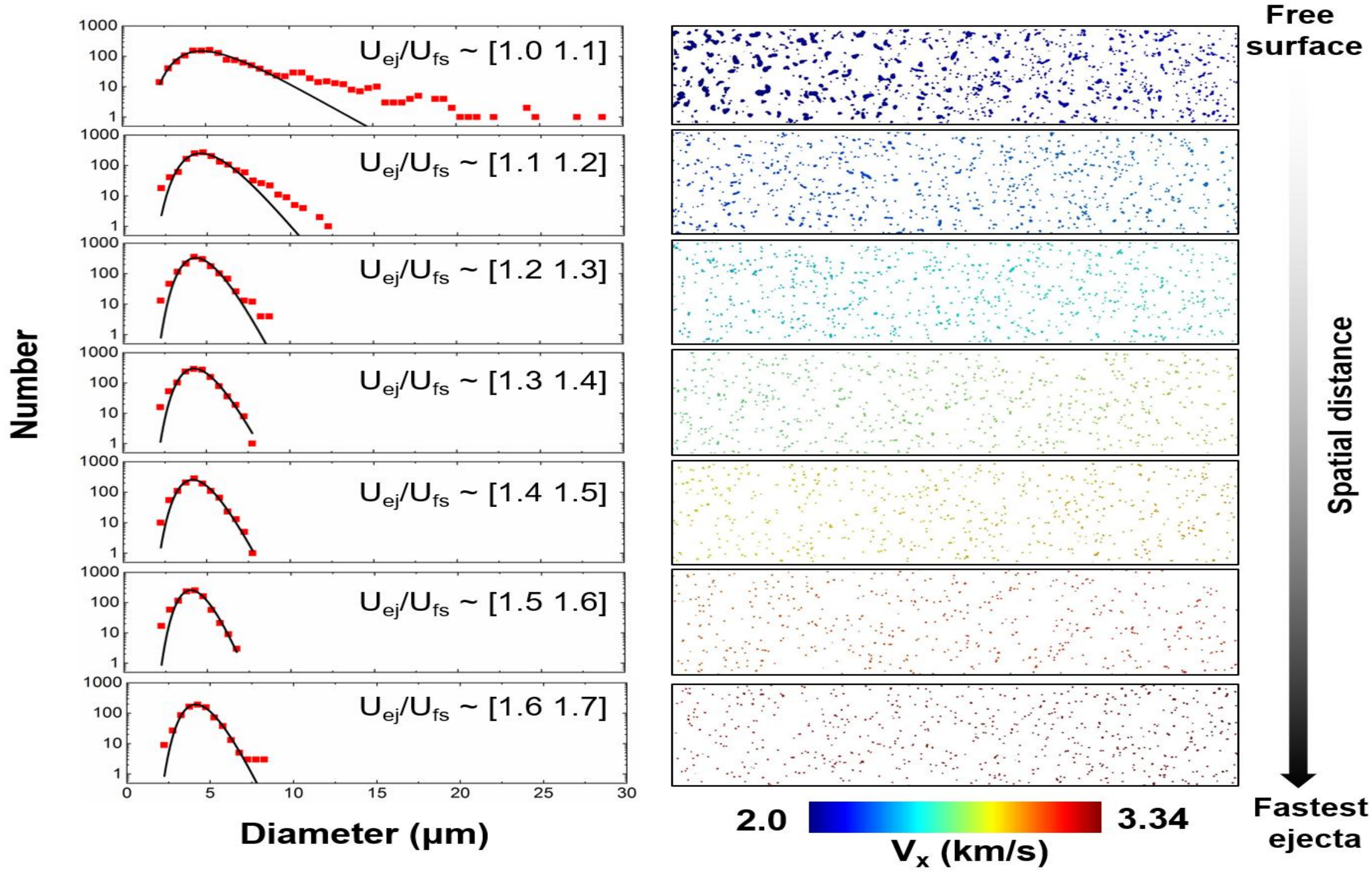

Particle Size in Different Spatial Regions

- The particle size decreases with the increase of spatial distance (or ejecta velocity);
- The particle size corresponding to the peak distribution has little change;

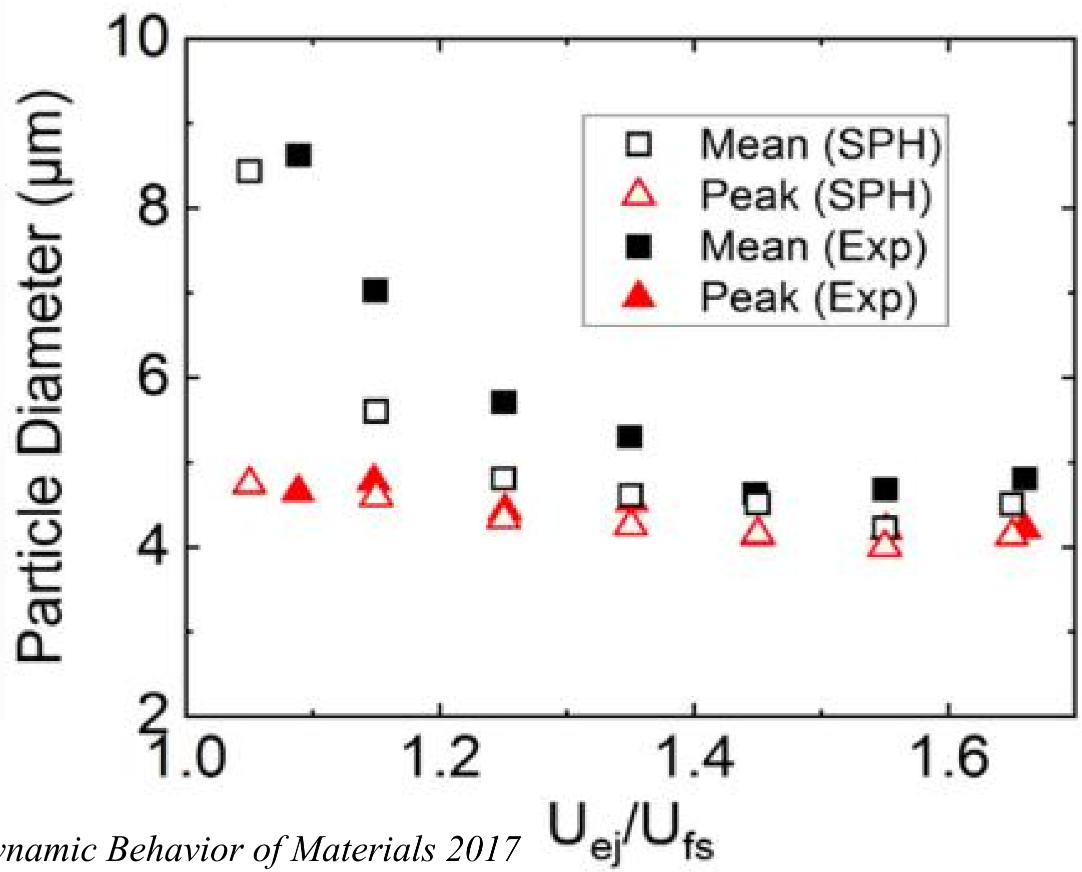

Sorenson et al. Journal of Dynamic Behavior of Materials 2017

Size Distributions

- The statistical law of particle size distribution **obeys a log normal distribution in small size while a power law in larger size**， in consistent with experiments;

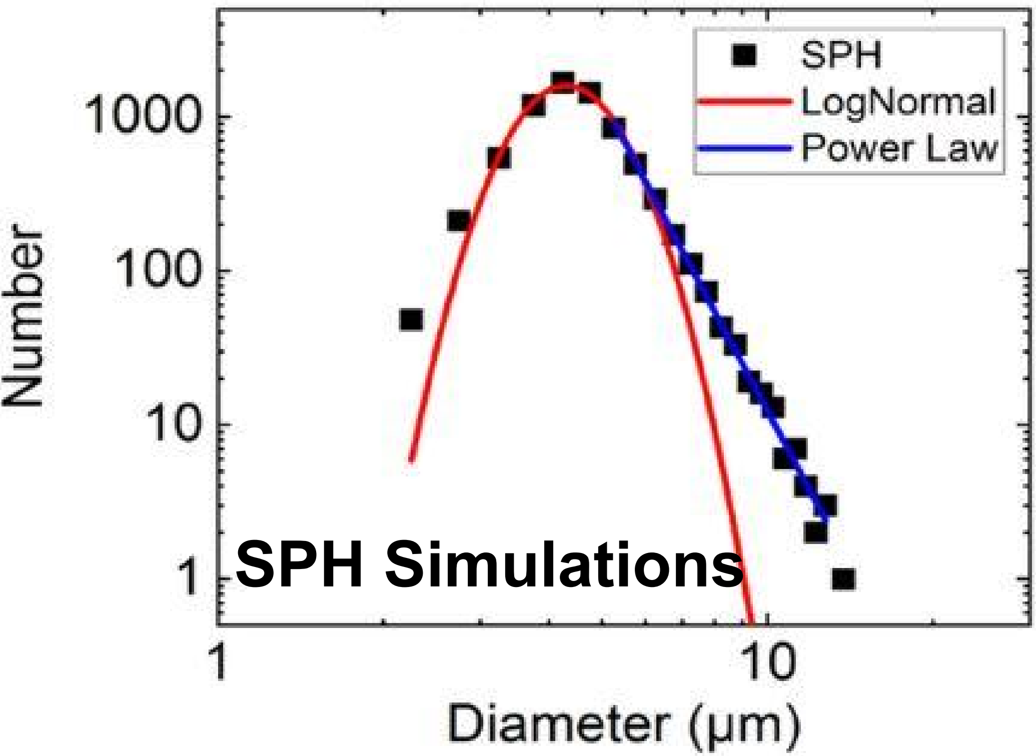

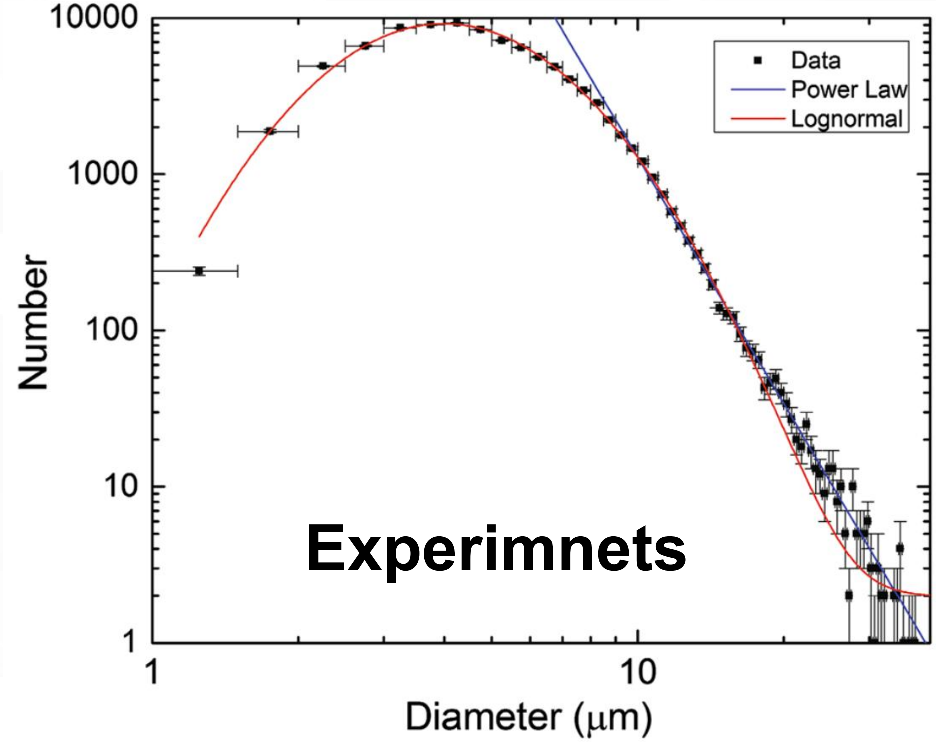

Sorenson D S, Journal of Dynamic Behavior of Materials, 2017

Images of Broken Particles

□ Comparison of Spatial Distribution Images of Broken Particles

strip structure

模拟

实验

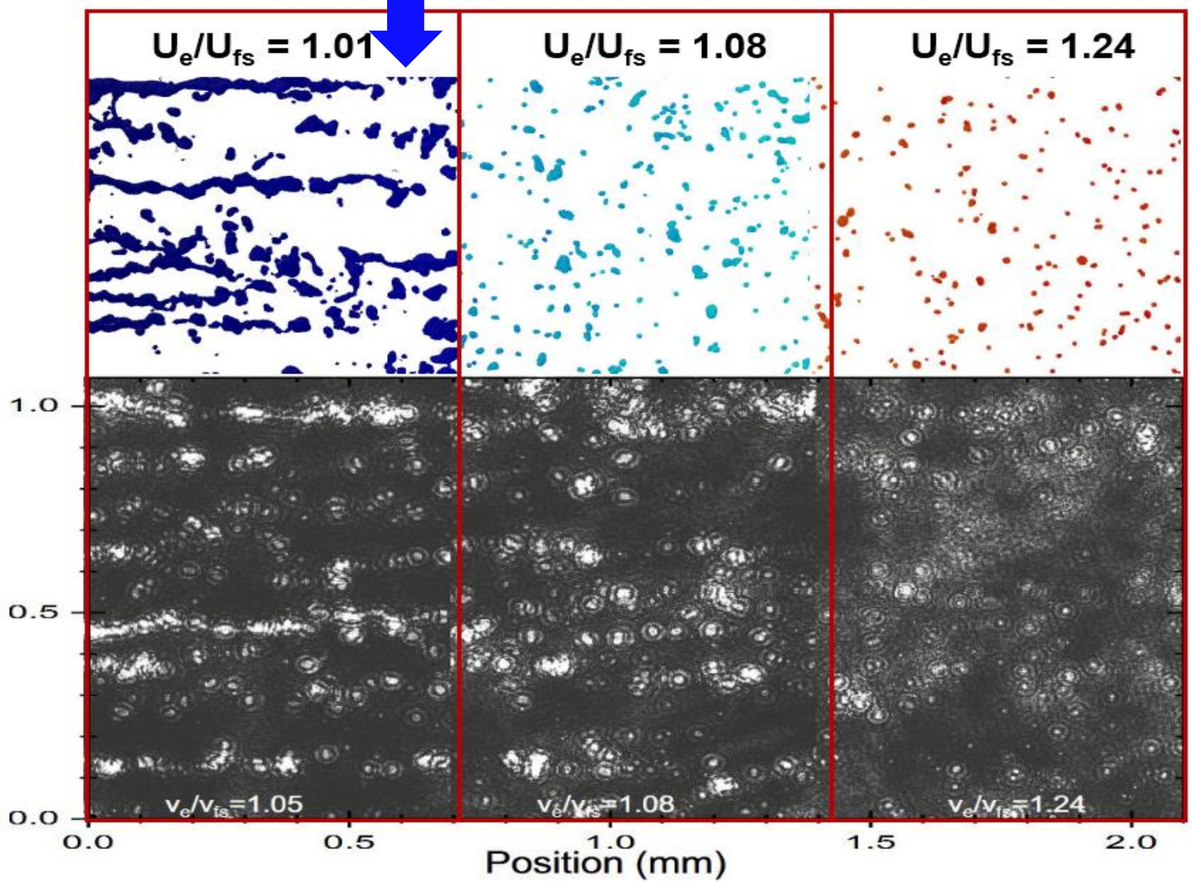

Sorenson et al. Journal of Dynamic Behavior of Materials 2017

Outline

- ✓ Background
- ✓ Numerical Methods
- ✓ Ejecta Breakup and Size distributions
- ✓ **Conclusions**

Conclusions

- A smooth particle hydrodynamics code with ability to simulate the long-term evolution of ejecta breakup;
- The dynamic fragmentation process of metal jet was simulated, and the particle calculation scale reached 130 million;
- The macroscopic dynamic evolution and particle size distribution of metal jet breakup are obtained, quantitative in agreement with experiments;

Bao Wu, Xin-Xin Wang, Pei Wang et al, Numerical investigation of shock-induced ejecta breakup and size distributions. (International Journal of Impact Engineering (2025) 105217

Thanks for your listening!